Nonlinear Dyn (2017) 89:2641–2655
DOI 10.1007/s11071-017-3613-z

ORIGINAL PAPER

Finite-time projective synchronization of memristor-based delay fractional-order neural networks

Mingwen Zheng · Lixiang Li · Haipeng Peng · Jinghua Xiao · Yixian Yang · Hui Zhao

Received: 22 December 2016 / Accepted: 9 June 2017 / Published online: 20 June 2017

Abstract This paper mainly investigates the finite-time projective synchronization problem of memristor-based delay fractional-order neural networks (MDFNNs). By using the definition of finite-time projective synchronization, combined with the memristor model, set-valued map and differential inclusion theory, Gronwall–Bellman integral inequality and Volterra-integral equation, the finite-time projective of MDFNNs is achieved via the linear feedback controller. Novel sufficient conditions are obtained to guarantee the finite-time projective synchronization of the drive-response MDFNNs. Besides, we also analyze the feasible region of the settling time. Finally, two numerical examples are given to show the effectiveness of the proposed results.

M. Zheng · J. Xiao · H. Zhao
School of Science, Beijing University of Posts and Telecommunications, Beijing 100876, China

M. Zheng
School of Science, Shandong University of Technology, Zibo 255000, China

J. Xiao
State Key Laboratory of Information Photonics and Optical Communications, Beijing University of Posts and Telecommunications, Beijing 100876, China

L. Li (✉) · H. Peng · Y. Yang
Information Security Center, State Key Laboratory of Networking and Switching Technology, Beijing University of Posts and Telecommunications, Beijing 100876, China
e-mail: Li_Lixiang2006@163.com

Keywords Finite-time projective synchronization · MDFNNs · Linear feedback controller · Volterra-integral equation

1 Introduction

The memristor is a new basic circuit element between charge and flux linkage proposed by Chua based on symmetry theory in 1971 [27]. In 2008, researchers at the HP laboratories created the memristor for the first time [43]. The most important difference between the memristor and the traditional resistance is that the resistance is dependent on the charge passing through it; therefore, it constantly changes its properties when an external signal passes. The memristor has a memory and can change information encoded by its resistance state. From this sense, the memristor is similar to the synapse of neurons in the brain. Scientists believe that the memristor is able to help us mimic a true neural network because of the freezing memory property [47]. So the memristor-based neural networks have attracted a lot of attention. More and more researchers build the memristor-based neural networks for a variety of application research, such as memristor-based neural networks modeling [3,22,34,56,57], data clustering using memristor networks [13], real-time encoding and compression [21], memristor-based associative memory neural networks [17,23], optimization and massively parallel computing [37,38], and machine learning [10].

Since German mathematician Leibniz discussed the concept of fractional calculus in 1695, fractional calculus has occupied the great mathematicians' time and has been studied for several centuries. The fractional calculus can be described as an extension of a derivative operator from integer order to arbitrary order. The fractional calculus equation is very suitable for characterizing materials and processes with memory and hereditary properties, and it has become one of the important tools in the mathematical modeling of the complex mechanical and physical processes. The study results show that the fractional-order differential systems can better model some natural phenomena. In fact, the chaotic behavior has been found in some fractional-order dynamical systems, such as fractional-order Lorenz system [20], fractional-order Rössler system [15], fractional-order Chen system [52], and so on. The above systems show chaotic behavior when the fractional order is less than 1. The discovery of this phenomenon makes researchers begin to pay attention to the synchronization and control of the neural networks when the nodes are fractional-order differential systems. Because of the unique advantages of fractional calculus, it has been widely used in viscoelastic materials [2,42], biology [30], molecular diffusion theory [26,32], seismic analysis [25,54], image processing [19], and control systems [9,29,39,51,59], etc. For example, Ref. [51] discussed chaos synchronization of fractional chaotic maps by applying the fractional difference based on the stability condition, and find that the chaotic signals studied in this paper are more sensitive because they are affected by both the initial values and the varied discretization time. With the emergence of memristor in recent years, the memristor-based fractional-order neural networks have been paid more and more attention, especially the study on stability and synchronization [4,14,28,41,48,58]. For example, Ma et al. [28] investigated the dynamical behavior composed memristor and improved Rössler oscillator and found both the nonlinear cross-terms and initial selection and resetting can be effective to control chaotic systems. This property can enhance the security of secure communication. Therefore, it is very valuable and practical to study memristor-based fractional-order neural networks.

Because of the limited speed of signal transmission between the neurons, the viscosity of synapses triggered by biological neural networks, and the finite switching speed between different circuit elements in hardware implementations of neural networks, time delay is a common phenomenon in neural networks. There are many types of delays, such as discrete delay, finite distributed delay, infinite distributed delay, neutral-type delay, and so on. The emergence of these delays is often the main reason for the oscillation, instability, and deteriorated performance of the dynamical systems. Therefore, the dynamic system with time delay becomes a hot topic in the theoretical and application realms.

Since Pecora and Carroll [35] showed that the synchronization of two chaotic systems with different initial conditions, the synchronization of various dynamic chaotic systems has become a research hot spot (see Refs. [8] and [36] for a review). Inspired by this, Mainieri and Rehacek [31] first proposed the concept of the projective synchronization, which the drive and response systems synchronize up to scale factor. Because of its proportional feature, the projective synchronization can realize faster communication through extending binary digital to M-nary digital [11]. Besides, the projective synchronization can be viewed as a general form of complete synchronization and anti-synchronization. Recently, some scholars have studied projective synchronization of fractional-order neural network with or without delay [4,44,49,55]. Wang et al. [49] investigated hybrid projective synchronization of fractional-order chaotic systems with time delay and realized the synchronization between two different structural chaotic systems using nonlinear controller; Velmurugan et al. [44] studied the hybrid projective synchronization of a fractional-order memristor-based neural networks with time delays; Bao et al. [4] investigated the projective synchronization of fractional-order memristor-based neural networks and derived some sufficient conditions by defining a Lyapunov function. However, to the best of our knowledge, there is not much research about the projective synchronization of memristor-based fractional-order neural networks.

Furthermore, the finite-time stability first proposed by Kamenkov [24] depicts a quantitative behavior of the system state variables in a specified finite-time interval. A system is said to be finite-time stable if the norm of its state variables is less than a certain boundary in a finite time when given any bounded initial value. Ref. [7] indicates that the finite-time stable system has faster convergence speed and better robustness. At present, although there are some studies on the finite-time stability and synchronization of fractional-

order neural networks [33,41,45,53,58], the finite-time projective synchronization of MDFNNS has not been reported to the best of our knowledge.

Motivated by the above discussion, the main objective of our paper is to investigate the finite-time projective synchronization of MDFNNs. With the aid of memristor mathematical model, set-valued map, differential inclusion, Gronwall–Bellman inequality, Volterra-integral equation, linear feedback controller, and the definition of finite-time projective synchronization, two new sufficient conditions are derived to ensure the finite-time projective synchronization of memristor-based fractional-order neural networks with or without time delay. The main contributions of this paper can be summarized as follows.

(1) We first investigate the finite-time projective synchronization of MDFNNs based on the proposed definition of finite-time projective synchronization according to the concept of the finite-time stability. The fractional-order differential equation is transformed into Volterra-integral equation, which simplifies our proof process of the main theorem.
(2) We obtain two sufficient conditions to guarantee the finite-time projective synchronization of the model used in this paper. Meanwhile, our results can be easily extended to the complete synchronization and anti-synchronization. Moreover, we analyze the feasible region of the settling time T_s, which can be calculated by solving a simple inequality condition.

The rest of this paper is organized as follows. The mathematical model of the memristor and the definition of fractional-order differential are introduced in Sect. 2. In Sect. 3, we describe the drive-response MDFNNs models, propose the definition of the finite-time projective synchronization, and introduce an assumption and two lemmas. Section 4 presents the main results of this paper, including two theorems and two corollaries. Two numerical examples are given to verify the correctness of main results in Sect. 5. Finally, we conclude the whole paper in Sect. 6.

Notations We define the norm of the vector as $\|a\| = \sum_{i=1}^{n} |a_i|$, and the norm of the matrix as $\|A\| = \max_j \sum_{i=1}^{n} |a_{ij}|$, respectively, where a_i and a_{ij} are the component of the vector a and the matrix A. $\mathbb{Z}^+$ are the sets of positive integer numbers, and $\mathbb{R}$ denotes the real set.

2 Preliminaries

In order to present our memristor-based delay fractional-order neural networks (MDFNNs), we need to prepare some knowledge about the mathematical model of the memristor and the fractional calculus.

2.1 Memristor model

According to the physical model of the HP memristor (see Fig. 1) [43], we have

$$\begin{aligned} v(t) &= \left(R_{\mathrm{ON}}\frac{w(t)}{D} + R_{\mathrm{OFF}}\left(1-\frac{w(t)}{D}\right)\right) i(t), \\ \frac{\mathrm{d}w(t)}{\mathrm{d}t} &= \frac{\mu_V R_{\mathrm{ON}}}{D} i(t) \end{aligned} \tag{1}$$

where D denotes the semiconductor film thicknesses, $w(t)$ is the state variable of the memristor, μ_V is aver-

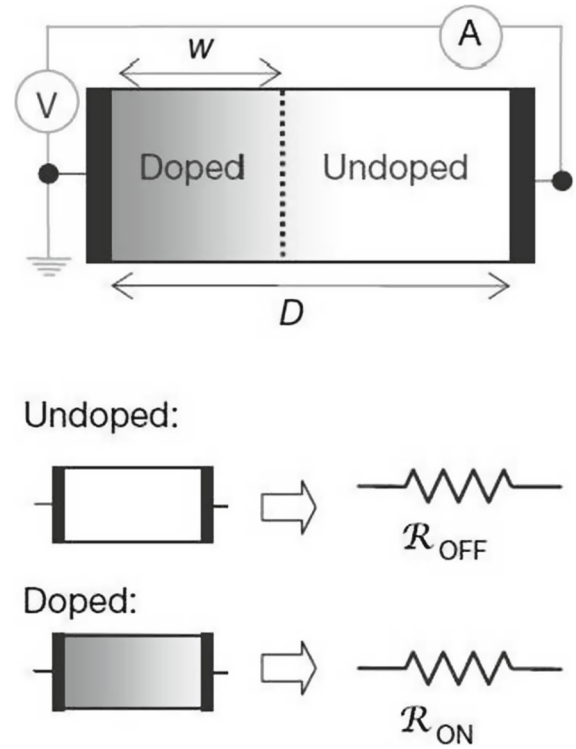

Fig. 1 Memistor diagram with a simplified equivalent circuit

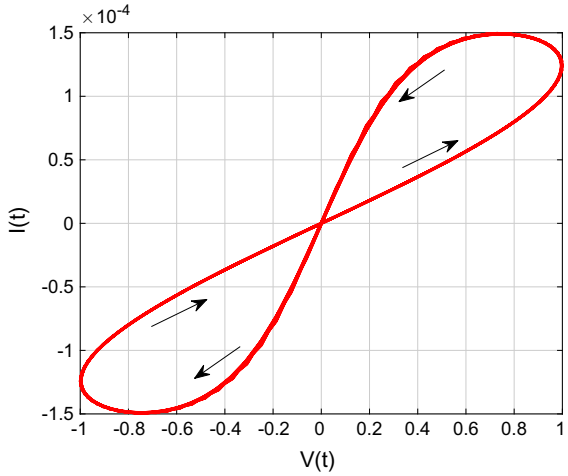

Fig. 2 The current–voltage characteristic of the memristor with a sinusoidal current

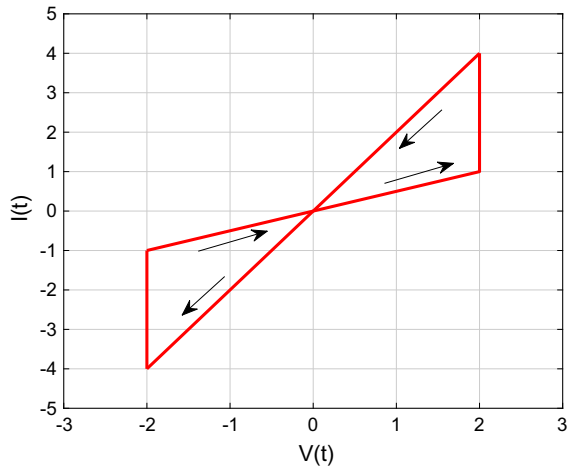

Fig. 3 The current–voltage characteristic of the surrogate memristor model

age ion mobility, $i(t)$ and $v(t)$ correspond to the current and voltage, respectively.

From Eq. (1), it yields the following equation for $w(t)$,

$$w(t) = \mu_V \frac{R_{\mathrm{ON}}}{D} q(t) \tag{2}$$

where $q(t)$ denotes the total charge passing through the memristor. According to Eq. (2), we obtain the calculation model of charge-controlled memristor

$$\begin{aligned} M(q) = \frac{v(t)}{i(t)} &= \mu_V \frac{R_{\mathrm{ON}}^2}{D^2} q(t) \\ &\quad + R_{\mathrm{OFF}} \left(1 - \frac{\mu_V R_{\mathrm{ON}}}{D^2} q(t)\right) \\ &\approx R_{\mathrm{OFF}} \left(1 - \frac{\mu_V R_{\mathrm{ON}}}{D^2} q(t)\right). \end{aligned} \tag{3}$$

The current–voltage characteristic of the memristor has significant pinched hysteresis loop fingerprint (see Fig. 2).

In order to simplify the mathematical model of the memristor on the premise of obtaining the pinched hysteresis feature, we select a surrogate memristor model (see Fig. 3) as follows [50]

$$M(v(t)) = \begin{cases} M_1(v(t)), |v(t)| \le T; \\ M_2(v(t)), |v(t)| > T. \end{cases} \tag{4}$$

2.2 Caputo fractional calculus

Since Leibniz and L'Hospital began to discuss fractional calculus in 1965, many famous mathematicians have given the definitions of fractional calculus from their different points of view. There are three well-known definitions of fractional calculus, which are given by Grünwald–Letnikov, Riemann-Liouville and Caputo, respectively. In contrast to the Grünwald–Letnikov and Riemann–Liouville fractional derivative, the Caputo fractional derivative has the following advantages: (1) it is not necessary to define the fractional-order initial conditions when solving fractional-order differential equations using Caputo's definition; (2) the derivative of a constant is 0 under the Caputo's definition; (3) it is integer-order derivative in the laplace transform of the fractional derivative using Caputo's definition. For these reasons, Caputo's definition is more commonly used in engineering and science. Next, we give the definition of Caputo's fractional calculus.

Definition 1 [40] The Caputo's fractional derivative of order q for a function $f(t) \in C^{n+1}([t_0, \infty], \mathbb{R})$ is defined as follows

$${}_{t_0}^{C} D_t^q f(t) = \frac{1}{\Gamma(n-q)} \int_{t_0}^{t} \frac{f^{(n)}(\tau)}{(t-\tau)^{q-n+1}} \mathrm{d}\tau. \tag{5}$$

where $n-1 < q < n, n \in \mathbb{Z}^+, t > t_0$, $\Gamma(\cdot)$ is the gamma function defined as $\Gamma(q) = \int_0^\infty t^{q-1} e^{-t} \mathrm{d}t$.

$C^{n+1}([t_0, \infty], \mathbb{R})$ denotes the set of all $n+1$ order continuous differentiable functions on the interval $[t_0, \infty]$.

In particular, when $0 < q < 1$, we have $n = 1$ and Eq. (5) can be rewritten as

$$ {}_{t_0}^{C}D_t^q f(t) = \frac{1}{\Gamma(1-q)} \int_{t_0}^{t} \frac{f'(\tau)}{(t-\tau)^q} \mathrm{d}\tau. \tag{6} $$

For the sake of simplicity, we use the symbol $D^q f(t)$ to denote the Caputo's fractional derivative.

2.3 The set-valued map and differential inclusion

For a differential system with discontinuous right-hand sides, Filippov gave a definition of differential inclusion solution, which can overcome the problem that the discontinuous solution cannot be given in the classical solution frame. The set-valued map theory provides the necessary basis for the study of differential inclusion problem.

Definition 2 [1] Let X and Y be two sets, a map $F : X \to Y$ is called set-valued map, if any $x \in X$, there is always a corresponding set $F(x) \subset Y$. $F(x)$ is said to the value or image of F at x.

Definition 3 [1] A set-valued map $F : X \to Y$ is said to be upper-semi-continuous at $x_0 \in X$, if for every neighborhood N_Y of $F(x_0) \subset Y$, there exists a neighborhood N_X of x_0 such that $F(N_X) = \bigcup_{x \in N_X} F(x) \subset N_Y$. If F is upper-semi-continuous for every $x \in X$, then the set-valued map F is upper-semi-continuous on the set X.

Consider the following differential equation system

$$ \begin{cases} \dot{x}(t) = g(x, t), \\ x_0 = x(t_0). \end{cases} \tag{7} $$

where $g(x, t)$ is discontinuous. And the Filippov solution of (7) is given as follows.

Definition 4 [18] A vector function $x(t)$ is a solution of the system (7) on $[t_0, t_1]$ in Filippov's sense, if $x(t)$ is absolutely continuous on any compact interval $[t_0, t_1]$ and for almost all $t \in [t_0, t_1]$ such that

$$ \dot{x} \in K_F[g](x, t), \tag{8} $$

where

$$ K_F[g](x, t) = \bigcap_{\delta > 0} \bigcap_{\mu(N)=0} \overline{co}\{g(\mathbb{B}_\delta(x)/N, t)\}. \tag{9} $$

In Eq. (9), $\overline{co}\{\cdot\}$ is the convex closure hull of a set, $\mathbb{B}_\delta(x) = \{y \| \|y - x\| \le \delta\}$ and $\mu(N)$ denotes the usual Lebesgue measure of set N.

3 Network models

We consider the drive-response synchronization problem of a class of memristor-based delay fractional-order neural networks (MDFNNs) described by the following two differential equations.

The drive system is expressed as follows

$$ \begin{cases} D^q x_i(t) = -c_i x_i(t) + \sum_{j=1}^{n} a_{ij}^{(1)}(x_j(t)) f_j(x_j(t)) \\ \quad + \sum_{j=1}^{n} b_{ij}^{(1)}(x_j(t-\tau)) g_j(x_j(t-\tau)) + I_i, \\ x_i(t) = \psi_i(t), t \in [-\tau, 0], i = 1, 2, \ldots, n. \end{cases} \tag{10} $$

The response system is expressed as follows

$$ \begin{cases} D^q y_i(t) = -c_i y_i(t) + \sum_{j=1}^{n} a_{ij}^{(2)}(y_j(t)) f_j(y_j(t)) \\ \quad + \sum_{j=1}^{n} b_{ij}^{(2)}(y_j(t-\tau)) g_j(y_j(t-\tau)) + I_i + u_i(t), \\ y_i(t) = \phi_i(t), t \in [-\tau, 0], i = 1, 2, \ldots, n. \end{cases} \tag{11} $$

where $x_i(t)$ and $y_i(t)$ denote the state variable associated with the ith neuron of drive and response system, respectively. $0 < q < 1$ is the fractional order, and τ is the time delay. $f(\cdot)$, $g(\cdot)$ are the activation functions without and with time delay, respectively. $c_i > 0$ denotes the self-feedback weight, and I_i is the external input bias value. $u_i(t)$ in the response system (11) is a linear feedback controller to be designed for making the drive-response system reach synchronization. The norm of the initial conditions of systems (10) and (11) is, respectively, $\|\psi(t)\| = \sup_{s \in [-\tau, 0]} |\psi(s)|$, and

$\|\phi(t)\| = \sup_{s\in[-\tau,0]}|\phi(s)|$. $a_{ij}^{(1)}(x_j(t))$, $a_{ij}^{(2)}(y_j(t))$ are memristive connection weights without time delay and $b_{ij}^{(1)}(x_j(t-\tau))$, $b_{ij}^{(2)}(y_j(t-\tau))$ are memristive connection weights with time delay. According to the characteristics of the current–voltage of the memristor, the connection weights satisfy the following conditions

$$\begin{aligned}
a_{ij}^{(1)}(x_j(t)) &= \begin{cases} \hat{a}_{ij}, |x_j(t)| \le T_j, \\ \check{a}_{ij}, |x_j(t)| > T_j, \end{cases} \\
a_{ij}^{(2)}(y_j(t)) &= \begin{cases} \hat{a}_{ij}, |y_j(t)| \le T_j, \\ \check{a}_{ij}, |y_j(t)| > T_j, \end{cases} \\
b_{ij}^{(1)}(x_j(t-\tau)) &= \begin{cases} \hat{b}_{ij}, |x_j(t-\tau)| \le T_j, \\ \check{b}_{ij}, |x_j(t-\tau)| > T_j, \end{cases} \\
b_{ij}^{(2)}(y_j(t-\tau)) &= \begin{cases} \hat{b}_{ij}, |y_j(t-\tau)| \le T_j, \\ \check{b}_{ij}, |y_j(t-\tau)| > T_j. \end{cases}
\end{aligned} \tag{12}$$

where the switching jumps $T_j > 0$, memristive connection weights $\hat{a}_{ij}, \check{a}_{ij}, \hat{b}_{ij}, \check{b}_{ij}, i, j = 1, 2, \ldots, n$ are constants.

From the above description, we can see that models (10) and (11) are complex switching systems with discontinuous right-hand side. Through the set-valued map and differential inclusions theory introduced in Sect. 2.3, we define the following set-valued maps

$$\begin{aligned}
K\left[a_{ij}^{(1)}(x_j(t))\right] &= \begin{cases} \hat{a}_{ij}, |x_j(t)| < T_j, \\ \overline{co}\{\hat{a}_{ij}, \check{a}_{ij}\}, |x_j(t)| = T_j, \\ \check{a}_{ij}, |x_j(t)| > T_j, \end{cases} \\
K\left[a_{ij}^{(2)}(y_j(t))\right] &= \begin{cases} \hat{a}_{ij}, |y_j(t)| < T_j, \\ \overline{co}\{\hat{a}_{ij}, \check{a}_{ij}\}, |y_j(t)| = T_j, \\ \check{a}_{ij}, |y_j(t)| > T_j, \end{cases} \\
K\left[b_{ij}^{(1)}(x_j(t-\tau))\right] &= \begin{cases} \hat{b}_{ij}, |x_j(t-\tau)| < T_j, \\ \overline{co}\{\hat{b}_{ij}, \check{b}_{ij}\}, |x_j(t-\tau)| = T_j, \\ \check{b}_{ij}, |x_j(t-\tau)| > T_j, \end{cases} \\
K\left[b_{ij}^{(2)}(y_j(t-\tau))\right] &= \begin{cases} \hat{b}_{ij}, |y_j(t-\tau)| < T_j, \\ \overline{co}\{\hat{b}_{ij}, \check{b}_{ij}\}, |y_j(t-\tau)| = T_j, \\ \check{b}_{ij}, |y_j(t-\tau)| > T_j, \end{cases}
\end{aligned} \tag{13}$$

where $i, j = 1, 2, \ldots, n, t > 0$.

Next, models (10) and (11) can be rewritten as a form of differential inclusions

$$\begin{aligned}
D^q x_i(t) \in & -c_i x_i(t) + \sum_{j=1}^{n} K\left[a_{ij}^{(1)}(x_j(t))\right] f_j(x_j(t)) \\
& + \sum_{j=1}^{n} K\left[b_{ij}^{(1)}(x_j(t-\tau))\right] g_j(x_j(t-\tau)) + I_i, \\
& i = 1, 2, \ldots, n
\end{aligned} \tag{14}$$

$$\begin{aligned}
D^q y_i(t) \in & -c_i y_i(t) + \sum_{j=1}^{n} K\left[a_{ij}^{(2)}(y_j(t))\right] f_j(y_j(t)) \\
& + \sum_{j=1}^{n} K\left[b_{ij}^{(2)}(y_j(t-\tau))\right] g_j(y_j(t-\tau)) + I_i, \\
& i = 1, 2, \ldots, n.
\end{aligned} \tag{15}$$

Or equivalently, there exist the measurable functions $\bar{a}_{ij}(t) \in K\left[a_{ij}^{(1)}(x_j(t))\right]$, $\bar{b}_{ij}(t) \in K\left[b_{ij}^{(1)}(x_j(t-\tau))\right]$, $\widetilde{a}_{ij}(t) \in K\left[a_{ij}^{(2)}(y_j(t))\right]$, $\widetilde{b}_{ij}(t) \in K\left[b_{ij}^{(2)}(y_j(t-\tau))\right]$ to make drive and response systems meet

$$\begin{cases}
D^q x_i(t) = -c_i x_i(t) + \sum_{j=1}^{n} \bar{a}_{ij}(t) f_j(x_j(t)) \\
\quad + \sum_{j=1}^{n} \bar{b}_{ij}(t) g_j(x_j(t-\tau)) + I_i, \\
x_i(t) = \psi_i(t), t \in [-\tau, 0], \\
i = 1, 2, \ldots, n.
\end{cases} \tag{16}$$

$$\begin{cases}
D^q y_i(t) = -c_i y_i(t) + \sum_{j=1}^{n} \widetilde{a}_{ij}(t) f_j(y_j(t)) \\
\quad + \sum_{j=1}^{n} \widetilde{b}_{ij}(t) g_j(y_j(t-\tau)) + I_i + u_i(t), \\
y_i(t) = \phi_i(t), t \in [-\tau, 0], \\
i = 1, 2, \ldots, n.
\end{cases} \tag{17}$$

The error system between the drive system (16) and the response system (17) is defined as

$$e_i(t) = y_i(t) - \alpha x_i(t). \tag{18}$$

where $\alpha \in \mathbb{R}$ is a real scaling factor. Especially, the initial condition of the error system is $e_i(t_0) = \phi_i(t) - \alpha\psi_i(t)$.

We select the following simple feedback controller

$$u_i(t) = -k_i(y_i(t) - \alpha x_i(t)). \tag{19}$$

where $k_i \in \mathbb{R}^+, i = 1, 2, \ldots, n$ is the control gain.

Definition 5 Under the controller (19), the drive system (16) and the response system (17) is said to be projective synchronization in finite time, if there exist positive numbers $\{t_0, J, \delta, \varepsilon\}, \delta < \varepsilon$, if and only if $\|e(t_0)\| < \delta$ implies $\|e(t)\| < \varepsilon, \forall t \in J = [t_0, t_0 + T]$, i.e., if the error system $\|e(t)\|$ is finite-time stable, the drive system (16) and the response system (17) can achieve the finite-time projective synchronization. Additionally, $T_s = T$ is called the finite settling time.

Remark 1 In Definition 5, the parameter ε stands for the set of all allowable states of the error system, and the parameter δ stands for the set of all initial states of the error system. Through Definition 5, we transform the projective synchronization problem into the stability problem of the error system.

In order to obtain our main results, we need the following an assumption and two lemmas.

Assumption 1 The activation functions $f_j(\cdot), g_j(\cdot)$ are Lipschitz continuous on $\mathbb{R}$, i.e., there exist positive constants m_j, l_j,

$$
\begin{aligned}
&|f_j(x) - f_j(y)| \le l_j|x - y|,\\
&|g_j(x) - g_j(y)| \le m_j|x - y|,\\
&x, y \in \mathbb{R}, j = 1, 2, \ldots, n.
\end{aligned}
$$

Lemma 1 *[12] Under Assumption 1, if $f_j(\pm T_j) = 0, j = 1, 2, \ldots, n$ then*

$$
\begin{aligned}
&|K\left[a_{ij}(x_j(t)\right] f_j(x_j(t)) - K\left[a_{ij}(y_j(t)) f_j(y_j(t))\right]\\
&\le \alpha_{ij}^u l_j \left|x_j(t) - y_j(t)\right|
\end{aligned}
$$

for $i, j = 1, 2, \ldots, n$, i.e., for any $\eta_{ij}(x_j(t)) \in K\left[a_{ij}(x_j(t)\right]$, $\eta_{ij}(y_j(t)) \in K\left[a_{ij}(y_j(t)\right]$,

$$
\begin{aligned}
&\left|\eta_{ij}(x_j(t)) f_j(x_j(t)) - \eta_{ij}(y_j(t)) f_j(y_j(t))\right|\\
&\le \alpha_{ij}^u l_j \left|x_j(t) - y_j(t)\right|.
\end{aligned}
$$

where $\alpha_{ij}^u = max\{\hat{a}_{ij}, \check{a}_{ij}\}$.

Lemma 2 *[5] Let $\lambda(t), \beta(t), u(t)$ be real-valued functions defined on an interval I. Assume that $\beta(t), u(t)$ are continuous and $\lambda(t)$ is integrable on $I = [t_0, t]$, $t_0 < t$, we have*

(1) If $\beta(t)$ is nonnegative and $u(t)$ satisfies the integral inequality

$$u(t) \le \lambda(t) + \int_a^t \beta(s)u(s)ds,$$

then

$$u(t) \le \lambda(t) + \int_a^t \lambda(s)\beta(s)exp\left(\int_s^t \beta(r)dr\right)ds,$$

(2) in addition, if $\lambda(t)$ is non-decreasing, then

$$u(t) \le \lambda(t)exp\left(\int_a^t \beta(s)ds\right).$$

4 Main results

In this section, we will derive the sufficient conditions for finite-time projective synchronization of the drive system (10) and the response system (11) using the Volterra-integral equation and Gronwall–Bellman inequality.

Theorem 1 *Under Assumption 1 and the linear feedback controller (19), the error system (18) of the drive system (16) and the response system (17) can achieve finite-time projective synchronization, when $\|e(t_0)\| = \|\Phi(t) - \alpha\Psi(t)\| < \delta$, where $\Phi(t) = (\phi_1(t), \phi_2(t), \ldots, \phi_n(t))^T, \Psi(t) = (\psi_1(t), \psi_2(t), \ldots, \psi_n(t))^T$, if the following sufficient condition holds*

$$
\begin{aligned}
&\left(1 + \frac{t^q - (t-\tau)^q}{\Gamma(q+1)}\right)\\
&\times exp\left(\frac{\left(\|\mathcal{AL} - \Lambda\| + \|\mathcal{BM}\|\right)}{\Gamma(q+1)}t^q\right) < \frac{\varepsilon}{\delta}.
\end{aligned}
\tag{20}
$$

where $\mathcal{A} = (a_{ij})_{n\times n}$, $\mathcal{B} = (b_{ij})_{n\times n}$, $\mathcal{M} = diag\{m_1, m_2, \ldots, m_n\}$, $\mathcal{L} = diag\{l_1, l_2, \ldots, l_n\}$.

Proof According the error system (18), we have

$$
\begin{aligned}
D^q e_i(t) &= D^q y_i(t) - D^q(\alpha x_i(t))\\
&= -c_i y_i(t) + \sum_{j=1}^n \bar{a}_{ij}(t) f_j(y_j(t))\\
&\quad + \sum_{j=1}^n \bar{b}_{ij}(t) f_j(y_j(t-\tau)) + I_i + u_i(t)
\end{aligned}
$$

$$
\begin{aligned}
&-\left(-c_i\alpha x_i(t)+\sum_{j=1}^{n}\widetilde{a}_{ij}(t)f_j(\alpha x_j(t))\right.\\
&\left.+\sum_{j=1}^{n}\widetilde{b}_{ij}(t)f_j(\alpha x_j(t-\tau))+I_i\right)\\
&=-(c_i+k_i)e_i(t)+\sum_{j=1}^{n}\bar{a}_{ij}(t)f_j(y_j(t))\\
&\quad-\sum_{j=1}^{n}\widetilde{a}_{ij}(t)f_j(\alpha x_j(t))+\sum_{j=1}^{n}\bar{b}_{ij}(t)f_j(y_j(t-\tau))\\
&\quad-\sum_{j=1}^{n}\widetilde{b}_{ij}(t)f_j(\alpha x_j(t-\tau)).
\end{aligned}
$$

Using Lemma 1, we have

$$
\begin{aligned}
D^q e_i(t) \;&\le -(c_i+k_i)e_i(t)+\sum_{j=1}^{n}a_{ij}l_j|e_j(t)|\\
&\quad+\sum_{j=1}^{n}b_{ij}m_j|e_j(t-\tau)|,
\end{aligned}
$$

where $a_{ij}=\max\{\hat{a}_{ij},\check{a}_{ij}\}$, $b_{ij}=\max\{\hat{b}_{ij},\check{b}_{ij}\}$.

For simplicity, we rewrite the above inequality into a vector form

$$
D^q e(t)\le -\Lambda e(t)+\mathcal{AL}|e(t)|+\mathcal{BM}|e(t-\tau)|, \quad (21)
$$

where $e(t)=(e_1(t),e_2(t),\ldots,e_n(t))^T$, $\Lambda=\mathrm{diag}\{c_1+k_1,c_2+k_2,\ldots,c_n+k_n\}$.

When $0<q<1$, Eq. (21) is equivalent to the following Volterra-integral equation

$$
\begin{aligned}
e(t)\le e(t_0)+\frac{1}{\Gamma(q)}\int_0^t(t-s)^{q-1}\,&(-\Lambda e(s)\\
&+\mathcal{AL}|e(s)|+\mathcal{BM}|e(s-\tau)|)\,\mathrm{d}s. \quad (22)
\end{aligned}
$$

Applying norm on both sides of Eq. (22), we can obtain

$$
\begin{aligned}
\|e(t)\| &\le \|e(t_0)\|+\frac{1}{\Gamma(q)}\int_0^t(t-s)^{q-1}\times\\
&\quad\|-\Lambda e(s)+\mathcal{AL}|e(s)|+\mathcal{BM}|e(s-\tau)|\|\mathrm{d}s\\
&\le \|e(t_0)\|+\frac{1}{\Gamma(q)}\int_0^t(t-s)^{q-1}\times\\
&\quad(\|\mathcal{AL}-\Lambda\|\|e(s)\|+\|\mathcal{BM}\|\|e(s-\tau)\|)\,\mathrm{d}s\\
&=\|e(t_0)\|+\frac{\|\mathcal{AL}-\Lambda\|}{\Gamma(q)}\int_0^t(t-s)^{q-1}\|e(s)\|\mathrm{d}s\\
&\quad+\frac{\|\mathcal{BM}\|}{\Gamma(q)}\int_0^t(t-s)^{q-1}\|e(s-\tau)\|\mathrm{d}s. \quad (23)
\end{aligned}
$$

By means of integral transformation and inequality amplification for Eq. (23), we have

$$
\begin{aligned}
&\int_0^t(t-s)^{q-1}\|e(s-\tau)\|\mathrm{d}s\\
&\overset{z=s-\tau}{=\!=}\int_{-\tau}^{t-\tau}(t-z-\tau)^{q-1}\|e(z)\|\mathrm{d}z\\
&=\int_{-\tau}^{t-\tau}(t-\tau-s)^{q-1}\|e(s)\|\mathrm{d}s\\
&\le\int_{-\tau}^{t}(t-\tau-s)^{q-1}\|e(s)\|\mathrm{d}s\\
&=\int_{-\tau}^{0}(t-\tau-s)^{\alpha-1}\|e(t_0)\|\mathrm{d}s\\
&\quad+\int_0^t(t-s)^{q-1}\|e(s)\|\mathrm{d}s\\
&=\frac{t^\alpha-(t-\tau)^q}{\alpha}\|e(t_0)\|\\
&\quad+\int_0^t(t-s)^{q-1}\|e(s)\|\mathrm{d}s.
\end{aligned} \quad (24)
$$

Substituting Eq. (24) into Eq. (23), we get

$$
\begin{aligned}
\|e(t)\| \;&\le\left(1+\tfrac{t^q-(t-\tau)^q}{\Gamma(q+1)}\right)\|e(t_0)\|\\
&\quad+\tfrac{1}{\Gamma(q)}\int_0^t\left(\|\mathcal{AL}-\Lambda\|+\|\mathcal{BM}\|\right)\\
&\quad\times(t-s)^{q-1}\|e(s)\|\mathrm{d}s \quad (25)
\end{aligned}
$$

Let $\lambda(t)=\left(1+\frac{t^q-(t-\tau)^q}{\Gamma(q+1)}\right)\|e(t_0)\|$, $\beta(t)=\frac{1}{\Gamma(q)}\left(\|\mathcal{AL}-\Lambda\|+\|\mathcal{BM}\|\right)(t-s)^{q-1}$. Obviously, $\lambda(t)$ is non-decreasing function when $t\ge 0$, according to Lemma 2, we can obtain

$$
\begin{aligned}
\|e(t)\| &\le \lambda(t)\exp(\int_0^t\beta(s))\mathrm{d}s\\
&=\left(1+\frac{t^q-(t-\tau)^q}{\Gamma(q+1)}\right)\|e(t_0)\|\\
&\quad\times\exp\left(\int_0^t\frac{1}{\Gamma(q)}\big(\|\mathcal{AL}-\Lambda\|\right.\\
&\quad\left.+\|\mathcal{BM}\|\big)(t-s)^{q-1}\big]\mathrm{d}s\right)\\
&=\left(1+\frac{t^q-(t-\tau)^q}{\Gamma(q+1)}\right)\|e(t_0)\|\\
&\quad\times\exp\left(\frac{\left(\|\mathcal{AL}-\Lambda\|+\|\mathcal{BM}\|\right)}{\Gamma(q+1)}t^q\right).
\end{aligned} \quad (26)
$$

From condition (20), we have $\|e(t)\|<\varepsilon$. According Definition 5, the error system (18) is finite-time stable,

thus, the MDFNNs (10) and (11) achieve the finite-time projective synchronization. The proof of Theorem 1 is completed.

Remark 2 We can calculate the finite settling time T_s by the condition (20). When the initial conditions and the fractional order are determined in the drive-response MDFNNs, and then given a ε, we can always obtain the settling time T_s by solving the inequality condition (20). Next, we will draw the feasible region of the settling time T_s. Given the corresponding parameter values, we plot the curves of the following equations in the Cartesian coordinates (see Fig. 4).

$$\begin{cases} y = f(t) = \left(1 + \dfrac{t^q - (t-\tau)^q}{\Gamma(q+1)}\right) \exp\left(\dfrac{(V)}{\Gamma(q+1)} t^q\right), \\ y = \dfrac{\varepsilon}{\delta}, \\ t = \tau. \end{cases}$$

From Fig. 4, we can see that the settling time T_s is affected by the initial value δ, delay τ and ε.

Remark 3 The results of Theorem 1 can be easily extended to the memristor-based fractional-order neural network without delay as shown below.

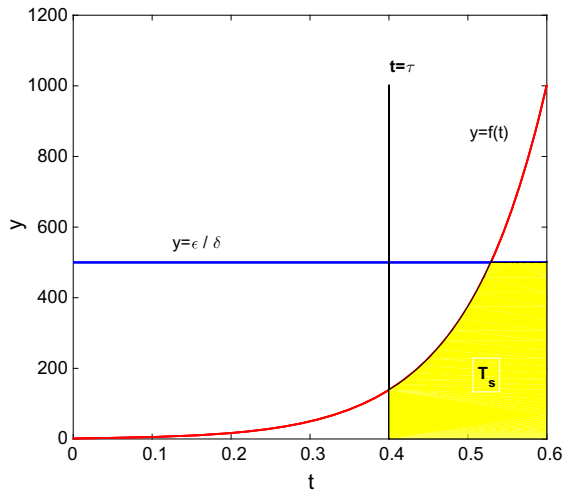

Fig. 4 The feasible area of the settling time T_s when the parameters are $V = 10, \delta = 2, \tau = 0.4, q = 0.9, \varepsilon = 1000, t = 0 : 0.01 : 0.6$

The drive system is expressed as follows

$$\begin{cases} D^q x_i(t) = -c_i x_i(t) + \sum_{j=1}^{n} a_{ij}^{(1)}(x_j(t)) f_j(x_j(t)) \\ \quad + I_i, \\ x_i(t) = \psi_i(t), t \in [-\tau, 0], \\ i = 1, 2, \ldots, n. \end{cases} \tag{27}$$

The response system is expressed as follows

$$\begin{cases} D^q y_i(t) = -c_i y_i(t) + \sum_{j=1}^{n} a_{ij}^{(2)}(y_j(t)) f_j(y_j(t)) \\ \quad + I_i + u_i(t), \\ y_i(t) = \phi_i(t), t \in [-\tau, 0] \\ i = 1, 2, \ldots, n. \end{cases} \tag{28}$$

Using the same analytical method of Theorem 1, we have the following result.

Theorem 2 *Under Assumption 1 and the linear feedback controller (19), the drive system (27) and the response system (28) can achieve projective synchronization, if the following condition holds*

$$exp\left(\frac{\|\mathcal{AL} - \Lambda\|}{\Gamma(q+1)} t^q\right) < \frac{\epsilon}{\delta}. \tag{29}$$

Proof The proof process is similar to that of Theorem 1 and is omitted here.

Remark 4 Although some references have studied the projection synchronization problem of fractional neural network with or without memristor [4,46,49,55], almost no one has studied the finite-time projective synchronization problem. Our approach provides a solution to the study of MDFNNs.

Remark 5 According to the different α values, the projective synchronization can also be extended to the investigation of the complete synchronization($\alpha = 1$) and anti-synchronization($\alpha = -1$) of the drive-response systems. So, we have the following two corollaries.

Corollary 1 *If the scaling factor $\alpha = 1$ in the error system (18) and the controller (19), under Assumption 1, the MDFNNs (10) and (11) can achieve the finite-time complete synchronization if the sufficient condition (20) holds.*

Corollary 2 *If the scaling factor $\alpha = -1$ in the error system (18) and the controller (19), under Assumption 1, the MDFNNs (10) and (11) can achieve the finite-time anti-synchronization if the sufficient condition (20) holds.*

5 Simulation examples

In this section, two numerical examples are given to show the effectiveness of our main results. We use the Predictor-Corrector method [6] to solve the approximate numerical solutions of the fractional-order delay differential equations.

Example 1 Consider the following three-dimensional memristor-based fractional-order neural networks without delays as the drive system

$$D^q x_i(t) = -c_i x_i(t) + \sum_{j=1}^{3} a_{ij}(x_j(t)) f(x_j(t)) + I_i, \quad i = 1, 2, 3. \tag{30}$$

The corresponding response system is given by

$$D^q y_i(t) = -c_i y_i(t) + \sum_{j=1}^{3} a_{ij}(y_j(t)) f(y_j(t)) + I_i + u_i(t), \quad i = 1, 2, 3. \tag{31}$$

All parameters of the drive system (30) and the response system (31) are selected as follows

$q = 0.95$, $C = \mathrm{diag}\{[1; 1; 1]\}$, $I = [0; 0; 0]$,
$x(0) = (-0.5, 0.3, 0.4)^T$, $y(0) = (0.5, 0.8, -0.4)^T$,
$f(x) = g(x) = \tanh(x)$,

$$a_{11}(x_1) = \begin{cases} 2.0, & |x_1| \le 1 \\ -2.0, & |x_1| > 1 \end{cases} \quad a_{12}(x_1) = \begin{cases} -1.0, & |x_1| \le 1 \\ 1.0, & |x_1| > 1 \end{cases}$$

$$a_{13}(x_1) = \begin{cases} 8.3, & |x_1| \le 1 \\ -8.3, & |x_1| > 1 \end{cases} \quad a_{21}(x_2) = \begin{cases} 6.8, & |x_2| \le 1 \\ -6.8, & |x_2| > 1 \end{cases}$$

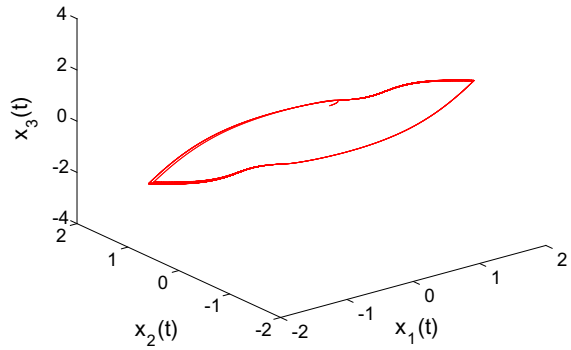

Fig. 5 Limit cycle of system (30) with initial value $x_0 = (-0.5, 0.3, 0.4)^T$

$$a_{22}(x_2) = \begin{cases} 1.5, & |x_2| \le 1 \\ -1.5, & |x_2| > 1 \end{cases} \quad a_{23}(x_2) = \begin{cases} -3.0, & |x_2| \le 1 \\ 3.0, & |x_2| > 1 \end{cases}$$

$$a_{31}(x_3) = \begin{cases} 1.8, & |x_3| \le 1 \\ -1.8, & |x_3| > 1 \end{cases} \quad a_{32}(x_3) = \begin{cases} -9.0, & |x_3| \le 1 \\ 9.0, & |x_3| > 1 \end{cases}$$

$$a_{33}(x_3) = \begin{cases} 1.2, & |x_3| \le 1 \\ -1.2, & |x_3| > 1. \end{cases}$$

Note: x_1 denotes $x_1(t)$ for simplicity.

Figure 5 shows that the drive system (30) has a limit cycle in the case of the above mentioned parameters. Taking the control gain $k_1 = k_2 = k_3 = 2$ in the controller (19), Lipschitz constants $l_1 = l_2 = l_3 = 1$, $\delta > \|e(0)\| = \|y(0) - \alpha x(0)\|$, α is scaling factor of projective synchronization. Figures 6, 7, 8 show the state trajectories when α is chosen a different value. According condition (29), let $\delta = 1.1 > \|e(0)\| = 1, \varepsilon = 7.7$, we can calculate the settling time $T_s = 0.2074$ when $\alpha = 3$.

Remark 6 We can see that the synchronization state errors do not stabilize to zeros from Fig. 9, but stable at a point less than $\varepsilon = 7.7$. The reason for this phenomenon is that we define the projective synchronization condition defined in Definition 5 is $\|e(t_0)\| < \varepsilon$. Obviously, Fig. 9 meets this condition. This proves the correctness of our results.

Remark 7 The settling time T_s calculated by the theory does not seem to agree with the actual running time. This is due to the simulation software (MATLAB R2016a) and the algorithms themselves (predictor-corrector PECE method of Adams–Bashforth–Moulton type [16]).

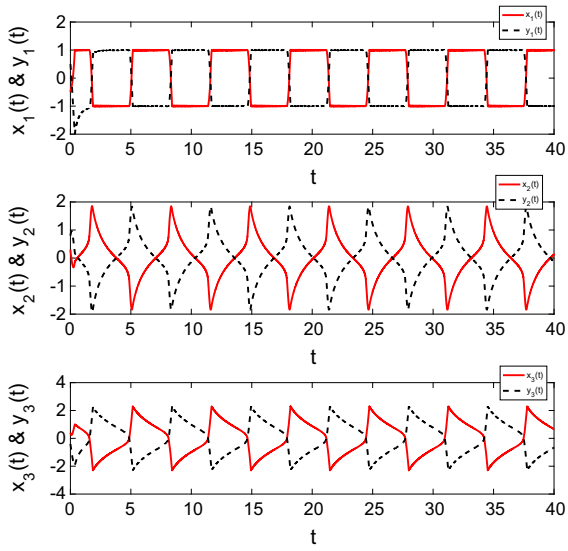

Fig. 6 (*Color online*) The state trajectories of $x(t)$, $y(t)$ when $\alpha = -1$

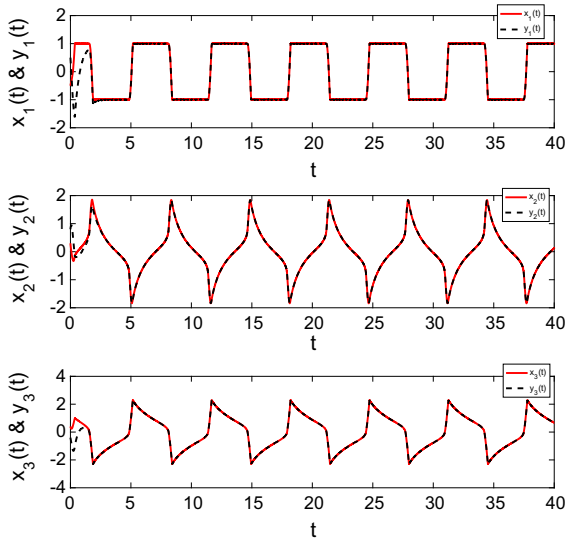

Fig. 7 (*Color online*) The state trajectories of $x(t)$, $y(t)$ when $\alpha = 1$

Figure 9 presents the synchronization error curves of the drive systems (30) and response system (31) when $\alpha = 3$.

Example 2 Consider the following two-dimensional memristor-based delay fractional-order neural networks as the drive system

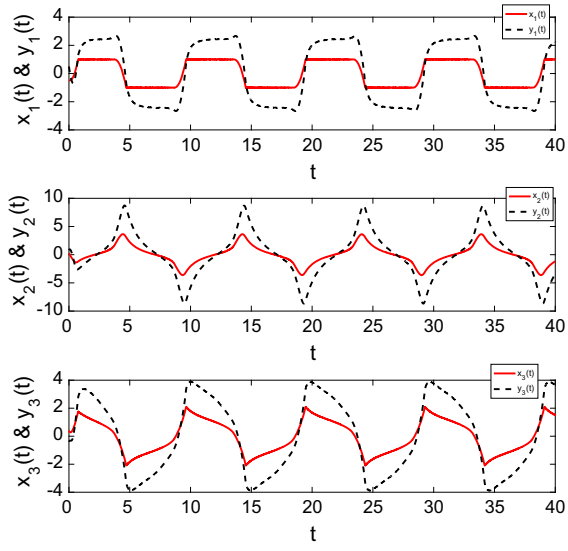

Fig. 8 (*Color online*) The state trajectories of $x(t)$, $y(t)$ when $\alpha = 3$

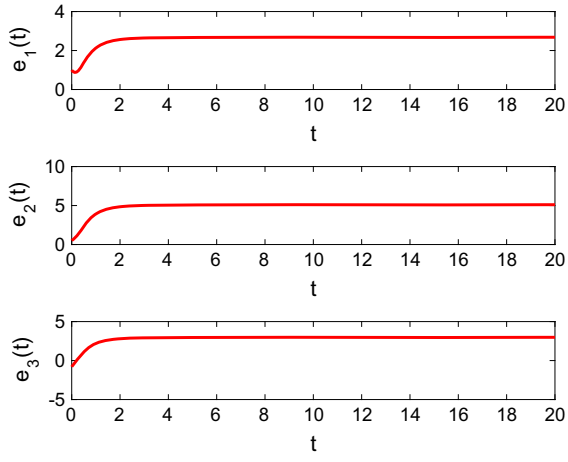

Fig. 9 The synchronization error curves of $x(t)$, $y(t)$ when $\alpha = 3$

$$D^q x_i(t) = -c_i x(t) + \sum_{j=1}^{2} a_{ij}(x_j(t)) f(x_j(t)) \sum_{j=1}^{2} b_{ij}(x_j(t-\tau)) g(x_j(t-\tau)) + I_i, i = 1, 2. \tag{32}$$

The corresponding response system is given by

$$D^q y_i(t) = -c_i y(t) + \sum_{j=1}^{2} a_{ij}(y_j(t)) f(y_j(t)) + \sum_{j=1}^{2} b_{ij}(y_j(t-\tau)) g(y_j(t-\tau)) + I_i + u_i(t), \quad i = 1, 2. \tag{33}$$

The parameters of the system (32) and (33) are listed below

$$q = 0.95,\ C = \mathrm{diag}\{[4; 2]\},\ I = [0; 0],$$
$$x(0) = (1.5, -0.8)^T,\ y(0) = (-1.5, 0.8)^T,$$
$$f(x) = g(x) = \tanh(x),\ \tau = 0.4,$$

$$a_{11}(x_1) = \begin{cases} 2.2, |x_1| \le 1 \\ 1.9, |x_1| > 1 \end{cases} \quad a_{12}(x_1) = \begin{cases} -2.0, |x_1| \le 1 \\ -3.0, |x_1| > 1 \end{cases}$$
$$a_{21}(x_2) = \begin{cases} -0.7, |x_2| \le 1 \\ -0.5, |x_2| > 1 \end{cases} \quad a_{22}(x_2) = \begin{cases} 2.5, |x_2| \le 1 \\ 2.8, |x_2| > 1 \end{cases}$$
$$b_{11}(x_1) = \begin{cases} -4.0, |x_1| \le 1 \\ -3.5, |x_1| > 1 \end{cases} \quad b_{12}(x_1) = \begin{cases} -2.5, |x_1| \le 1 \\ -2.8, |x_1| > 1 \end{cases}$$
$$b_{21}(x_2) = \begin{cases} -1.5, |x_2| \le 1 \\ -1.8, |x_2| > 1 \end{cases} \quad b_{22}(x_2) = \begin{cases} -3.5, |x_2| \le 1 \\ -3.8, |x_2| > 1. \end{cases}$$

Note: for simplicity, $a_{ij}(x_j)$ denotes $a_{ij}(x_j(t))$, and $b_{ij}(x_j)$ denotes $b_{ij}(x_j(t-\tau))$, $i, j = 1, 2$.

Figure 10 illustrates that the drive system (32) has a limit cycle when taking the parameters above. Taking

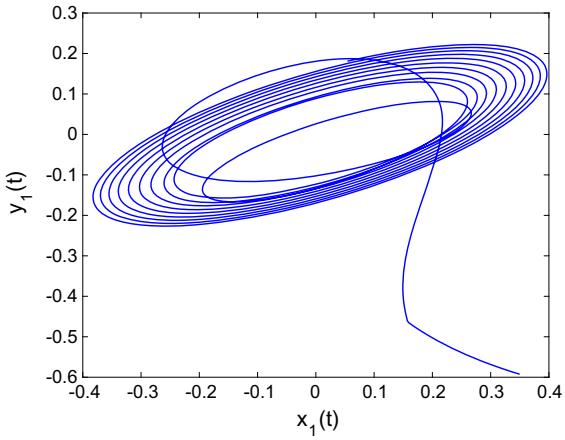

Fig. 10 Limit cycle of system (32) with initial value $x_0 = (-0.5, 0.3, 0.4)^T$

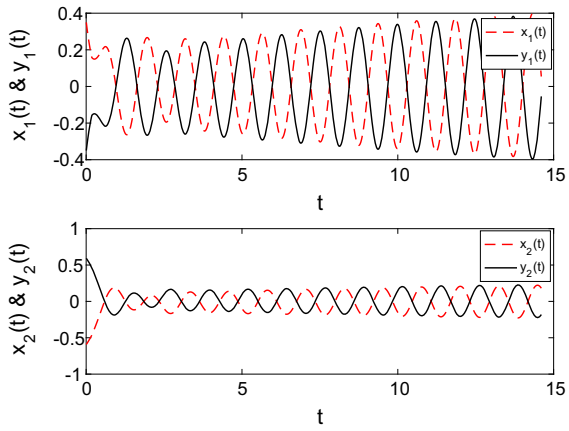

Fig. 11 (*Color online*) The state trajectories of $x(t)$, $y(t)$ when $\alpha = -1$

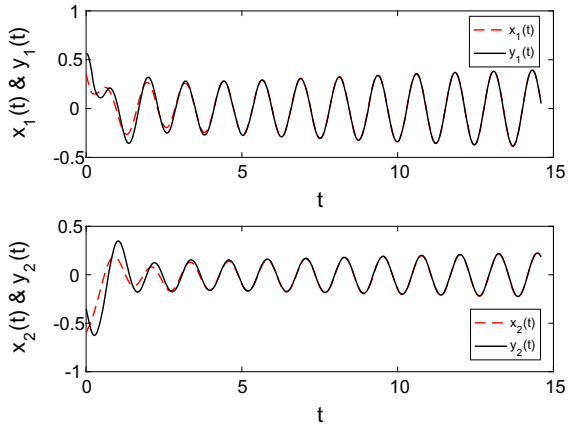

Fig. 12 (*Color online*) The state trajectories of $x(t)$, $y(t)$ when $\alpha = 1$

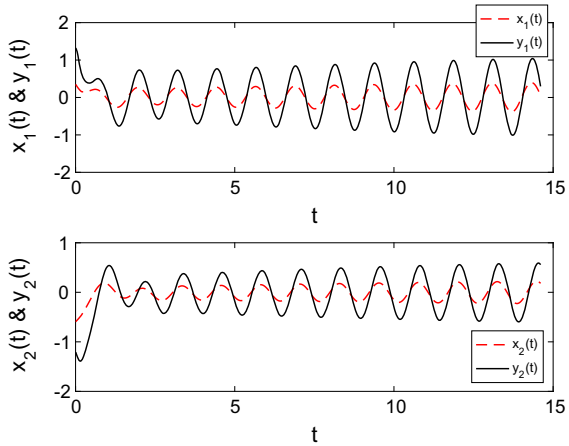

Fig. 13 (*Color online*) The state trajectories of $x(t)$, $y(t)$ when $\alpha = 3$

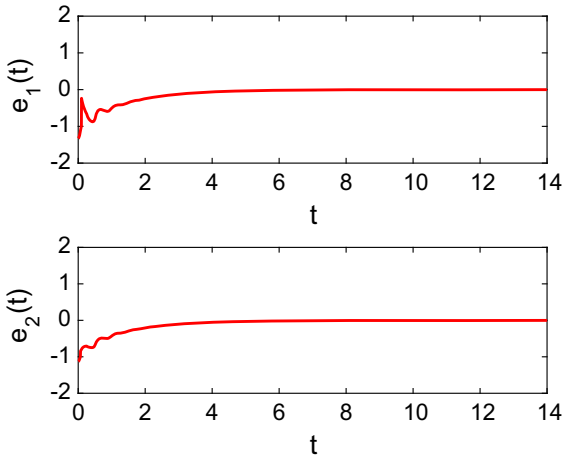

Fig. 14 The synchronization *error curves* of $x(t)$, $y(t)$ when $\alpha = 3$

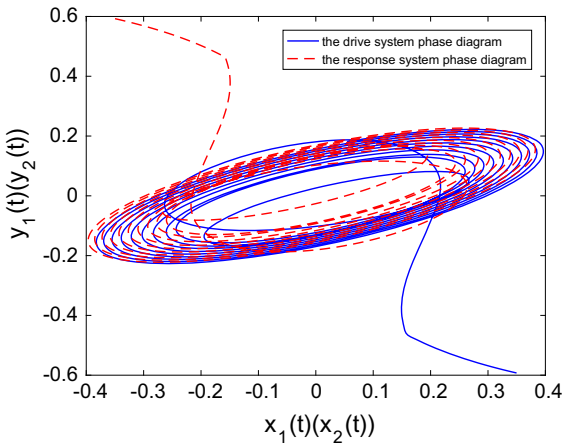

Fig. 15 (*Color online*) The phase diagram of the drive-response systems (32), (33) when $\alpha = -1$

the control gain $k_1 = 4, k_2 = 2$ in the controller (19), Lipschitz constants $l_1 = l_2 = 1, m_1 = m_2 = 1$. Thus, we have $\delta > \|e(0)\| = \|y(0) - \alpha x(0)\|$, α is the scaling factor of projective synchronization. Figures 11, 12, 13 show the state trajectories when $\alpha = -1, 1, 3$, respectively. Figure 14 depicts the synchronization error curves of the drive system (32) and the response system (33) when $\alpha = 3$. According the condition (20), let $\delta = 6.1 > \|e(0)\| = 6$, $\varepsilon = 3000$, we can calculate the settling time $T_s = 0.4186$.

Remark 8 In order to make the inequality condition (20) always holds, besides choosing an appropriate ε, we also need to ensure $t - \tau \geq 0$.

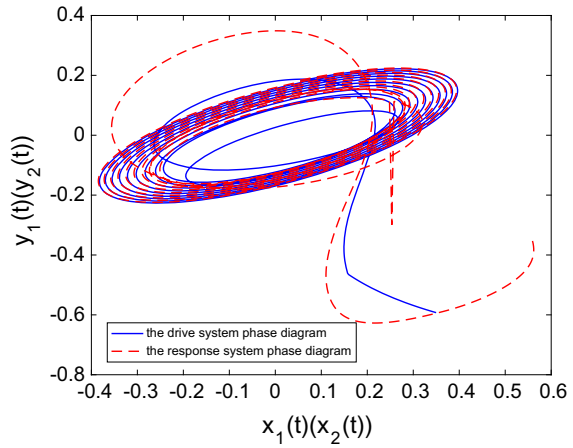

Fig. 16 (*Color online*) The phase diagram of the drive-response systems (32), (33) when $\alpha = 1$

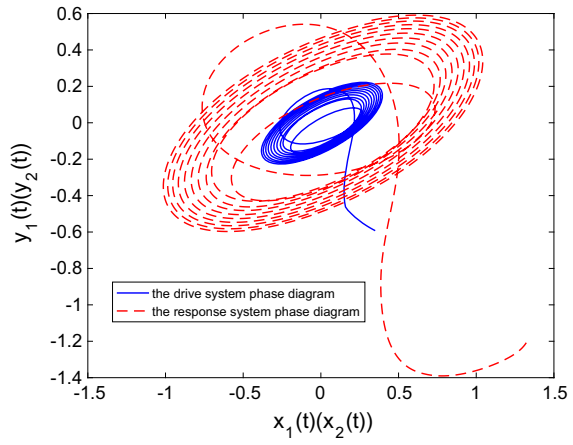

Fig. 17 (*Color online*) The phase diagram of the drive-response systems (32), (33) when $\alpha = 3$

In this example, we also draw the phase diagrams of the drive-response systems when $\alpha = -1, 1, 3$ as shown in Figs. 15, 16, 17.

6 Conclusions

The finite-time projective synchronization problem of MDFNNs is studied based on the definition of finite-time projective synchronization. Using the memristor model, fractional-order differential, the set-valued map, differential inclusion theory, Gronwall–Bellman inequality, and Volterra-integral equation of the fractional-order error system between the drive system and the response system, we derive the suf-

ficient conditions of the projective synchronization of MDFNNs under a simple linear feedback controller. We analyze the feasible region of the settling time. Meanwhile, our results can be easily extended to the cases of complete synchronization and anti-synchronization. The proof of the main theorem is simple, and the sufficient conditions are easy to verify. Moreover, we may calculate the settling time by these sufficient conditions. Finally, Two numerical examples have been presented to show the correctness of our results. The future work mainly includes the following aspects: (1) how to analyze the projective synchronization of more complex fractional-order neural network model with stochastic perturbation and various time delays, such as time-varying delays, infinite distributed delays and neutral-type delays; (2) how to derive the fixed-time synchronization conditions of MDFNNs. In summary, the fractional-order neural networks still have a lot of problems worthy of further study.

Acknowledgements This paper is supported by the National Key Research and Development Program (Grant No.2016YFB 0800602), the National Natural Science Foundation of China (Grant Nos.61472045, 61573067).

References

1. Aubin, J.P., Frankowska, H.: Set-Valued Analysis. Springer, Berlin (2009)
2. Bagley, R.L., Torvik, P.: A theoretical basis for the application of fractional calculus to viscoelasticity. J. Rheol. **27**(3), 201–210 (1983)
3. Bao, H., Park, J.H., Cao, J.: Adaptive synchronization of fractional-order memristor-based neural networks with time delay. Nonlinear Dyn. **82**(3), 1343–1354 (2015)
4. Bao, H.B., Cao, J.D.: Projective synchronization of fractional-order memristor-based neural networks. Neural Netw. **63**, 1–9 (2015)
5. Bellman, R., et al.: The stability of solutions of linear differential equations. Duke Math. J. **10**(4), 643–647 (1943)
6. Bhalekar, S., Daftardar-Gejji, V.: A predictor–corrector scheme for solving nonlinear delay differential equations of fractional order. J. Fract. Calc. Appl. **1**(5), 1–9 (2011)
7. Bhat, S.P., Bernstein, D.S.: Finite-time stability of continuous autonomous systems. SIAM J. Control Optim. **38**(3), 751–766 (2000)
8. Boccaletti, S., Kurths, J., Osipov, G., Valladares, D., Zhou, C.: The synchronization of chaotic systems. Phys. Rep. **366**(1), 1–101 (2002)
9. Caponetto, R., Dongola, G., Fortuna, L., Petráš, I.: Fractional Order Systems: Modeling and Control Applications. World Scientific Series on Nonlinear Science. World Scientific, Singapore (2010)
10. Carbajal, J.P., Dambre, J., Hermans, M., Schrauwen, B.: Memristor models for machine learning. Neural Comput. **27**(3), 725 (2015)
11. Chee, C., Xu, D.: Chaos-based m-ary digital communication technique using controlled projective synchronisation. IEE Proc. Circuits Devices Syst. **153**(4), 357–360 (2006)
12. Chen, J., Zeng, Z., Jiang, P.: Global Mittag-Leffler stability and synchronization of memristor-based fractional-order neural networks. Neural Netw. **51**, 1–8 (2014)
13. Choi, S., Sheridan, P., Lu, W.D.: Data clustering using memristor networks. Sci. Rep. **5**, 10492 (2015)
14. Cui, X., Yu, Y., Wang, H., Hu, W.: Dynamical analysis of memristor-based fractional-order neural networks with time delay. Mod. Phys. Lett. B **30**(18), 1650271 (2016)
15. Dadras, S., Momeni, H.R., Qi, G., Wang, Z.L.: Four-wing hyperchaotic attractor generated from a new 4d system with one equilibrium and its fractional-order form. Nonlinear Dyn. **67**(2), 1161–1173 (2012)
16. Diethelm, K., Freed, A.D.: The fracpece subroutine for the numerical solution of differential equations of fractional order. Forschung und wissenschaftliches Rechnen **1999**, 57–71 (1998)
17. Duan, S., Zhang, Y., Hu, X., Wang, L., Li, C.: Memristor-based chaotic neural networks for associative memory. Neural Comput. Appl. **25**(6), 1437–1445 (2014)
18. Filippov, A.F.: Differential Equations with Discontinuous Righthand Sides: Control Systems, vol. 18. Springer, Berlin (2013)
19. Ghamisi, P., Couceiro, M.S., Benediktsson, J.A., Ferreira, N.M.: An efficient method for segmentation of images based on fractional calculus and natural selection. Expert Syst. Appl. **39**(16), 12407–12417 (2012)
20. Grigorenko, I., Grigorenko, E.: Chaotic dynamics of the fractional Lorenz system. Phys. Rev. Lett. **91**(3), 034101 (2003)
21. Gupta, I., Serb, A., Khiat, A., Zeitler, R., Vassanelli, S., Prodromakis, T.: Real-time encoding and compression of neuronal spikes by metal-oxide memristors. Nat. Commun. **7**, 12805 (2016)
22. Hernández-Mejía, C., Sarmiento-Reyes, A., Vázquez-Leal, H.: A novel modeling methodology for memristive systems using homotopy perturbation methods. Circuits Syst. Signal Process. **36**(3), 1–22 (2016)
23. Hu, X., Duan, S., Chen, G., Chen, L.: Modeling affections with memristor-based associative memory neural networks. Neurocomputing **223**(5), 129–137 (2016)
24. Kamenkov, G.: On stability of motion over a finite interval of time. J. Appl. Math. Mech. **17**(2), 529–540 (1953)
25. Koh, C.G., Kelly, J.M.: Application of fractional derivatives to seismic analysis of base-isolated models. Earthq. Eng. Struct. Dyn. **19**(2), 229–241 (1990)
26. Lenzi, E., dos Santos, M., Lenzi, M., Vieira, D., da Silva, L.: Solutions for a fractional diffusion equation: anomalous diffusion and adsorption–desorption processes. J. King Saud Univ. Sci. **28**(1), 3–6 (2016)
27. Leon, C.: Memristor-the missing circuit element. IEEE Trans. Circuit Theory **18**(5), 507–519 (1971)
28. Ma, J., Wu, F., Ren, G., Tang, J.: A class of initials-dependent dynamical systems. Appl. Math. Comput. **298**, 65–76 (2017)

29. Machado, J.T.: Analysis and design of fractional-order digital control systems. Syst. Anal. Model. Simul. **27**(2–3), 107–122 (1997)
30. Magin, R.L.: Fractional calculus models of complex dynamics in biological tissues. Comput. Math. Appl. **59**(5), 1586–1593 (2010)
31. Mainieri, R., Rehacek, J.: Projective synchronization in three-dimensional chaotic systems. Phys. Rev. Lett. **82**(15), 3042 (1999)
32. Metzler, R., Klafter, J.: The random walk's guide to anomalous diffusion: a fractional dynamics approach. Phys. Rep. **339**(1), 1–77 (2000)
33. Mobayen, S.: Finite-time tracking control of chained-form nonholonomic systems with external disturbances based on recursive terminal sliding mode method. Nonlinear Dyn. **80**(1–2), 669–683 (2015)
34. Naous, R., Al-Shedivat, M., Salama, K.N.: Stochasticity modeling in memristors. IEEE Trans. Nanotechnol. **15**(1), 15–28 (2016)
35. Pecora, L.M., Carroll, T.L.: Synchronization in chaotic systems. Phys. Rev. Lett. **64**(8), 821 (1990)
36. Pecora, L.M., Carroll, T.L.: Synchronization of chaotic systems. Chaos Interdiscip. J. Nonlinear Sci. **25**(9), 097611 (2015)
37. Pershin, Y.V., Di Ventra, M.: Solving mazes with memristors: a massively parallel approach. Phys. Rev. E **84**(4), 046703 (2011)
38. Pershin, Y.V., La Fontaine, S., Di Ventra, M.: Memristive model of amoeba learning. Phys. Rev. E **80**(2), 021926 (2009)
39. Petráš, I.: Fractional-order nonlinear controllers: design and implementation notes. In: Proceedings of the IEEE ICCC2016, High Tatras, Slovak Republic (2016)
40. Podlubny, I.: Fractional Differential Equations, vol. 198. Academic press, New York (1998)
41. Rakkiyappan, R., Velmurugan, G., Cao, J.: Finite-time stability analysis of fractional-order complex-valued memristor-based neural networks with time delays. Nonlinear Dyn. **78**(4), 2823–2836 (2014)
42. Sapora, A., Cornetti, P., Carpinteri, A., Baglieri, O., Santagata, E.: The use of fractional calculus to model the experimental creep-recovery behavior of modified bituminous binders. Mater. Struct. **49**(1–2), 45–55 (2016)
43. Strukov, D.B., Snider, G.S., Stewart, D.R., Williams, R.S.: The missing memristor found. Nature **453**(7191), 80–83 (2008)
44. Velmurugan, G., Rakkiyappan, R.: Hybrid projective synchronization of fractional-order memristor-based neural networks with time delays. Nonlinear Dyn. **83**(1–2), 419–432 (2016)
45. Wang, B., Ding, J., Wu, F., Zhu, D.: Robust finite-time control of fractional-order nonlinear systems via frequency distributed model. Nonlinear Dyn. **85**(4), 2133–2142 (2016)
46. Wang, F., Yang, Y., Hu, M., Xu, X.: Projective cluster synchronization of fractional-order coupled-delay complex network via adaptive pinning control. Phys. A Stat. Mech. Appl. **434**, 134–143 (2015)
47. Wang, F.Z., Helian, N., Wu, S., Yang, X., Guo, Y., Lim, G., Rashid, M.M.: Delayed switching applied to memristor neural networks. J. Appl. Phys. **111**(7), 07E317 (2012)
48. Wang, L., Shen, Y., Yin, Q., Zhang, G.: Adaptive synchronization of memristor-based neural networks with time-varying delays. IEEE Trans. Neural Netw. Learn. Syst. **26**(9), 2033–2042 (2015)
49. Wang, S., Yu, Y., Wen, G.: Hybrid projective synchronization of time-delayed fractional order chaotic systems. Nonlinear Anal. Hybrid Syst. **11**, 129–138 (2014)
50. Wu, A., Zeng, Z.: Dynamic behaviors of memristor-based recurrent neural networks with time-varying delays. Neural Netw. **36**, 1–10 (2012)
51. Wu, G.C., Baleanu, D., Xie, H.P., Chen, F.L.: Chaos synchronization of fractional chaotic maps based on the stability condition. Phys. A Stat. Mech. Appl. **460**, 374–383 (2016)
52. Wu, X., Lu, Y.: Generalized projective synchronization of the fractional-order chen hyperchaotic system. Nonlinear Dyn. **57**(1), 25–35 (2009)
53. Xiao, J., Zhong, S., Li, Y., Xu, F.: Finite-time Mittag-Leffler synchronization of fractional-order memristive BAM neural networks with time delays. Neurocomputing **219**, 431–439 (2017)
54. Xu, J., Wang, D., Dang, C.: A marginal fractional moments based strategy for points selection in seismic response analysis of nonlinear structures with uncertain parameters. J. Sound Vib. **387**, 226–238 (2017)
55. Yu, J., Hu, C., Jiang, H., Fan, X.: Projective synchronization for fractional neural networks. Neural Netw. **49**, 87–95 (2014)
56. Zha, J., Huang, H., Liu, Y.: A novel window function for memristor model with application in programming analog circuits. IEEE Trans. Circuits Syst. II Express Briefs **63**(5), 423–427 (2016)
57. Zhang, Y., Wang, X., Li, Y., Friedman, E.G.: Memristive model for synaptic circuits. IEEE Trans. Circuits Syst. II Express Briefs (2016). doi:10.1109/TCSII.2016.2605069
58. Zheng, M., Li, L., Peng, H., Xiao, J., Yang, Y., Zhao, H.: Finite-time stability and synchronization for memristor-based fractional-order Cohen–Grossberg neural network. Eur. Phys. J. B **89**(9), 204 (2016)
59. Zhou, P., Ding, R., Cao, Y.X.: Multi drive-one response synchronization for fractional-order chaotic systems. Nonlinear Dyn. **70**(2), 1263–1271 (2012)